

# Symmetry of carrier-envelope phase difference effects in strong-field, few-cycle ionization of atoms and molecules

Christian Per Juul Martiny and Lars Bojer Madsen

*Department of Physics and Astronomy, University of Aarhus, 8000 Århus C, Denmark*

(Dated: July 28, 2018)

In few-cycle pulses, the exact value of the carrier-envelope phase difference (CEPD) has a pronounced influence on the ionization dynamics of atoms and molecules. We show that for atoms in circularly polarized light, a change in the CEPD is mapped uniquely to an overall rotation of the system, and results for arbitrary CEPD are obtained by rotation of the results from a single calculation with fixed CEPD. For molecules this is true only for linear molecules aligned parallel with the propagation direction of the field. The effects of CEPD are classified as geometric or non-geometric. The observations are exemplified by strong-field calculations on hydrogen.

PACS numbers: 32.80.Rm, 33.80.Rv, 42.50.Hz.

Nowadays, it is possible to construct and control intense laser pulses with only a few optical cycles [1], i.e., pulses described by a vector potential of the form  $\vec{A}(t) = A_0 f(t) \sin(\omega(t - \frac{\tau}{2}) + \phi) \hat{e}$ , where  $A_0$  is the amplitude,  $f(t)$  is the envelope,  $\tau$  is the pulse length,  $\omega$  is the frequency,  $\phi$  is the carrier-envelope phase difference (CEPD), and  $\hat{e}$  is the polarization vector. The corresponding electric field is obtained from the vector potential by  $\vec{E}(t) = -\partial_t \vec{A}(t)$ , and is shown in Fig. 1 for a  $\sin^2$  envelope. Such pulses can be used to probe molecular and atomic dynamics on a very short time scale [2, 3]. The associated ionization dynamics becomes sensitive to the exact shape of the pulse and the carrier-envelope phase difference (CEPD) (see Fig. 1). This dependence may be understood by the exponential dependence of the ionization rate on the instantaneous field strength and the corresponding emergence of the electron into the field-dressed continuum at specific instants of time during the pulse [4]. Asymmetries in the photoelectron spectrum may give information about the CEPD, and hence help in the characterization of the field. Electrons released at different times are accelerated to different final momenta and this fact is exploited in attosecond streaking [5] to map the time distribution of the pulse into a momentum distribution of the photoelectron, and to characterize the ultra-fast pulses [6]. Hence, just as few-cycle pulses are diagnostic tools for atoms and small molecules, the very same systems serve as diagnostic tools for the pulses themselves [7]. The latter statement, of course, assumes that an accurate theoretical description is at hand for the pulsed laser-matter interaction. It is the purpose of this work to add further to this understanding. In particular we are concerned with the CEPD effects, and a geometric interpretation of these.

Carrier-envelope phase difference effects were studied theoretically with emphasis on CEPD-induced spatial asymmetries in the ATI-spectrum/angular distribution in a number of papers on strong-field ionization of atoms [8, 9, 10, 11, 12] and molecules [13], strong-field dissociation [14], and high-harmonic generation [15]. The

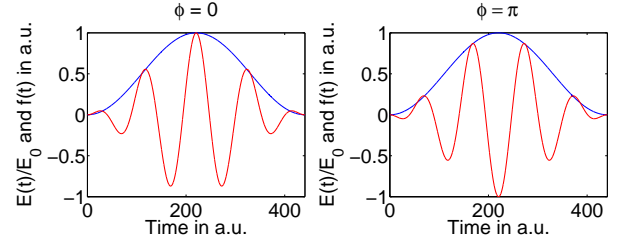


FIG. 1: (Color online). The electric field  $E(t)/E_0$ , normalized to the peak field strength  $E_0$  and the pulse envelope  $f(t)$  as a function of time for two values of the CEPD,  $\phi$ . The electric field points in opposite directions for  $\phi = 0$  and  $\phi = \pi$ . In ionization, the electric field will shake the electron until it gains enough energy to escape the Coulomb potential, and the angular distribution will depend on CEPD because the electric field (and the force  $\vec{F} = -\vec{E}$ ) points in opposite directions for  $\phi = 0$  and  $\phi = \pi$ . The field parameters are  $\tau = 441$  a.u. and  $\omega = 0.057$  a.u. (800 nm).

asymmetries can be used to extract information about and ultimately to measure the CEPD. In Ref. [16] a spatial asymmetry in ionization with few-cycle circular polarized laser pulses was observed for the first time. In Ref. [17] the generation of intense few-cycle laser pulses with stable CEPD was demonstrated, and a way of measuring CEPD, based on soft-X-ray radiation was presented. In Ref. [18] a spatial asymmetry in the ionization with few-cycle linear polarized laser pulses was measured, and the CEPD was determined with an estimated error of  $\pi/10$ . Asymmetries in the ionization signal combined with an attosecond pump pulse [6] were used to measure directly the field of a linearly polarized few-cycle pulse [7]. Very recently, the detailed control over the CEPD played a crucial role in attosecond electron dynamics [18, 19, 20], and experiments supporting the present findings have been reported at conferences [21].

In this work, we present a systematic theoretical study of the symmetry of the response of atomic and molecular systems under a change of the CEPD in few-cycle pulses,

and we exemplify the discussion with a study of the differential electron momentum distribution for hydrogen under such pulses.

We start out by considering an  $n$ -electron atom interacting with a few-cycle circularly polarized laser pulse described by the vector potential

$$\vec{A}(\phi, t, \vec{r}) = \frac{A_0}{\sqrt{2}} f(\eta) \times \left( \cos(\eta + \phi + \frac{\pi}{2}) \vec{e}_x + \sin(\eta + \phi + \frac{\pi}{2}) \vec{e}_y \right), \quad (1)$$

with  $f(\eta) = \sin^2(\frac{\eta}{2N})$  the envelope,  $N$  the number of optical cycles,  $\eta = \omega t - k z$ ,  $\omega$  the frequency, and  $\vec{k} = k \vec{e}_z$  the wave vector. In the present case, with full inclusion of the spatial dependence of the field, the interaction of the atom with the field is obtained by the minimal coupling  $\hat{p} \rightarrow \hat{p} + \vec{A}$  and the time-dependent Schrödinger equation reads [atomic units (a.u.) with  $m_e = e = a_0 = \hbar = 1$  are used throughout],

$$i \frac{\partial}{\partial t} \Psi = \left( H_0 + \sum_{j=1}^n \vec{A}(\phi, t, \vec{r}_j) \cdot \hat{p}_j + \frac{n A_0^2}{4} f^2(\eta) \right) \Psi, \quad (2)$$

where  $H_0$  is the field-free Hamiltonian. We are interested in relating this equation to an equation for the  $\phi = 0$  case. To this end, we note that the unitary operator  $D(\phi) = \exp(i J_z \phi)$ , where  $J_z$  is the total angular momentum, corresponds to a rotation of our system by an angle  $-\phi$  around the  $z$ -axis. Since  $H_0$  is invariant under rotations around the  $z$ -axis, the transformed wave function  $\Psi' = D(\phi) \Psi$  satisfies the Schrödinger equation,

$$i \frac{\partial}{\partial t} \Psi' = \left( H_0 + \sum_{j=1}^n D(\phi) \vec{A}(\phi, t, \vec{r}_j) \cdot \hat{p}_j D^\dagger(\phi) + \frac{n A_0^2}{4} D(\phi) f^2(\eta) D^\dagger(\phi) \right) \Psi', \quad (3)$$

and using the Baker-Hausdorff lemma [22] we obtain,

$$i \frac{\partial}{\partial t} \Psi' = \left( H_0 + \sum_{j=1}^n \vec{A}(0, t, \vec{r}_j) \cdot \hat{p}_j + \frac{n A_0^2}{4} f^2(\eta) \right) \Psi'. \quad (4)$$

When we compare (2) and (4), we see that a change in the CEPD from  $\phi = 0$  to  $\phi = \phi'$  corresponds to a rotation of our system around the  $z$ -axis by the angle  $\phi'$ . This fact is not only theoretically interesting, but also helpful in practical calculations since this symmetry property reduces the number of computations one has to perform to a single one – all other results are obtained by suitable rotations. For instance, imagine we are interested in the differential ionization probability  $\frac{dP_{fi}}{dq_x dq_y}(\phi)$  for the momenta  $q_x, q_y$  in the polarization plane and for a general  $\phi > 0$ . Then we calculate  $\frac{dP_{fi}}{dq_x dq_y}(\phi = 0)$ , and rotate the result counterclockwise by an angle  $\phi$  to obtain  $\frac{dP_{fi}}{dq_x dq_y}(\phi)$ .

In the above derivation it is essential that the field-free Hamiltonian  $H_0$  is invariant to rotations around the  $z$ -axis. If this is not the case, the proof breaks down. As an example we look at ionization of diatomic molecules, or more generally linear molecules, in circularly polarized few-cycle laser pulses. If the molecule is aligned along the laser propagation direction, then the field-free Hamiltonian still has the required symmetry and the theorem holds. If the molecule is not aligned along this axis, the system does not have the required symmetry and CEPD effects can not be reduced to a geometrical rotation. Accordingly, we may make a distinction between rotational invariant atomic and molecular systems where the CEPD effects are purely geometric rotations, and systems which are not rotational invariant in which case true *non-geometrical* CEPD effects occur. For example, the results on strong-field ionization of  $K_2^+$  with the molecule in the polarization plane [13] belong to the latter category.

As an illustration of the present findings, we consider ionization of atomic hydrogen,  $H(1s)$ , in the strong-field approximation (SFA) [23]. We assume the dipole approximation which means that  $\eta = \omega t$  in (1) and use that  $\vec{E} = -\partial_t \vec{A}$ . The probability amplitude for direct ionization reads

$$T_{fi} = -i \int_0^\tau \langle \Psi_f(\vec{r}, t) | \vec{E} \cdot \vec{r} | \Psi_i(\vec{r}, t) \rangle dt, \quad (5)$$

where  $\Psi_i(\vec{r}, t)$  is the  $1s$  ground state wave function. The final state  $\Psi_f(\vec{r}, t)$  is represented by a Coulomb-Volkov wave function [24] with asymptotic momentum  $\vec{q}$ . The integral in (5) is analyzed as in [24] and the numerical evaluation is performed with Gauss-Legendre quadrature. By exploiting the invariance of the dot-product under rotations ( $\vec{E}(\phi) \cdot \vec{r} = [R_z(\phi) \vec{E}(\phi = 0)] \cdot [R_z(\phi) R_z(-\phi) \vec{r}] = \vec{E}(\phi = 0) \cdot \vec{r}'$ , where  $R_z(\phi)$  is the  $3 \times 3$  matrix describing rotations around the  $z$  axis), the SFA is readily shown to respond to CEPD changes like the exact theory discussed above.

Once  $T_{fi}$  is known, a simple numerical integration over  $q_z$  gives us the  $(q_x, q_y)$  distribution  $\frac{dP_{fi}}{dq_x dq_y} = \int |T_{fi}|^2 dq_z$ . Figure 2 presents the calculated distribution for various values of  $\phi$ . For varying  $\phi$ , the distribution rotates in accordance with the general theory. For  $\phi = 0$ ,  $\frac{dP_{fi}}{dq_x dq_y}$  has a peak around  $(q_x = 0, q_y \sim 0.6)$  (this peak corresponds to about 14 photons above threshold), and is almost symmetric around the line  $q_x = 0$ . As  $\phi$  increases, this line is turned counterclockwise, so that  $\frac{dP_{fi}}{dq_x dq_y}$  has a peak around  $(q_y = 0, q_x \sim -0.6)$  for  $\phi = \frac{\pi}{2}$ .

Some of the features can be explained by a semiclassical two-step model [11]: first the electron escapes to the continuum at  $t = t_0$  with velocity  $\vec{v}(t_0) = \vec{0}$ . Second, it moves like a classical particle under the influence of the external Coulomb and laser fields. If, we neglect the Coulomb potential, which is justified if the

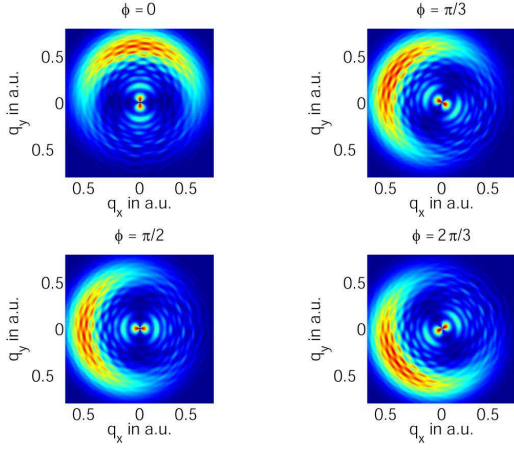


FIG. 2: (Color online) The  $(q_x, q_y)$  distribution for strong-field ionization of H(1s) for various values of  $\phi$ , with  $I = 5.0 \times 10^{13} \text{ W/cm}^2$ ,  $\omega = 0.057$  corresponding to a central wavelength of 800nm and three cycles,  $N = 3$ . The grid size is  $dq_x = dq_y = 0.01$ .

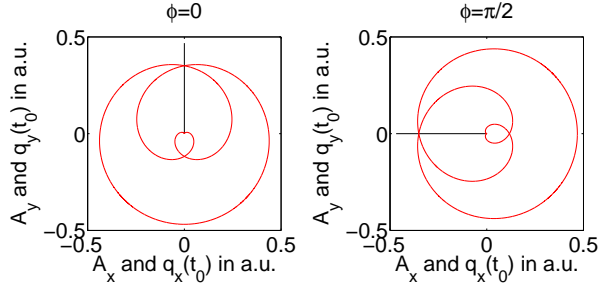


FIG. 3: The curves show the time-dependent vector potential and the lines show  $\vec{q}^d$  for  $\phi = 0, \pi/2$ . Laser parameters are as in Fig. 2.

field is very strong, Newton's second law tells us that  $q_x(t) = A_x(t) + q_x^d$ ,  $q_y(t) = A_y(t) + q_y^d$  where  $q_x^d = -A_x(t_0)$  and  $q_y^d = -A_y(t_0)$ . This means that the photoelectron direction, after the pulse where  $\vec{A}$  vanishes, is determined by the vector  $\vec{q}^d = (q_x^d, q_y^d)$ . For simplicity  $t_0$  is chosen to be  $\tau/2$ , which is the time when  $|\vec{E}(t)|$  reaches its maximum. Figure 3 shows plots of the time-dependent vector potential and  $\vec{q}^d = -\vec{A}(t_0)$  for various values of  $\phi$ . The model explains how the preferred direction (the line of symmetry) of the photoelectron depends on CEPD.

Finally we consider the case of a linearly polarized laser field and return to the question of symmetry. The vector potential in the linear case,  $\vec{A}(\phi, t, \vec{r}) = A_0 f(\eta) \sin(\eta + \phi + \pi/2) \hat{e}_y$ , can be written as  $\vec{A}(\phi, t, \vec{r}) = \frac{1}{\sqrt{2}} (\vec{A}_L(\phi, t) - \vec{A}_R(\phi, t))$ , where  $\vec{A}_{L/R}(\phi, t, \vec{r}) = \frac{A_0}{\sqrt{2}} f(\eta) (\cos(\eta + \phi + \pi/2) \hat{e}_x \pm \sin(\eta + \phi + \pi/2) \hat{e}_y)$  describe left (+) and right (-) hand circularly polarized fields. This relation suggests that we can characterize CEPD effects for a linearly po-

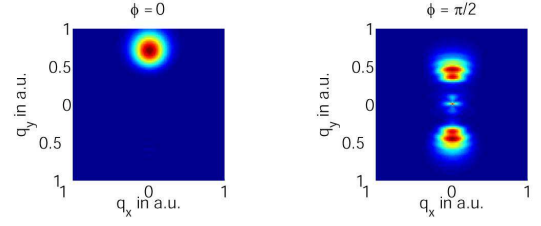


FIG. 4: (Color online) The  $(q_x, q_y)$  distribution for strong-field ionization of H(1s) by a linearly polarized field for  $\phi = 0, \pi/2$ , with  $I = 5.0 \times 10^{13} \text{ W/cm}^2$ ,  $\omega = 0.057$  corresponding to a central wavelength of 800nm and three cycles,  $N = 3$ . The grid size is  $dq_x = dq_y = 0.02$ .

larized pulse similarly to circularly polarized pulses. Unfortunately, in exact theory, it is not possible to separate the effects of the circularly polarized fields, since they do not individually commute with the field-free Hamiltonian.

Figure 4 shows two examples for a linear field corresponding to the  $\phi = 0$  and  $\phi = \pi/2$  cases. These results may be interpreted in terms of the classical model discussed above ( $q_y = -A_y(t_0)$ ). For  $\phi = 0$ , the vector potential peaks in the negative  $y$  direction at the peak of the envelope and produces electrons with positive momentum,  $q_y = -A_y(\frac{\tau}{2})$ . For  $\phi = \pi/2$ , the vector potential is anti-symmetric with respect to the peak of the envelope, and the electron spectrum reflects this in a forward-backward symmetry. For  $\phi = \pi/2$ , the spectrum has moved to smaller momenta since the two maxima of the vector potential are lower in this case. Notice, however, that the model can not explain the size of the shift. There are two reasons for this discrepancy. First, the model neglects the Coulomb potential. Second we assume that  $v_0 = 0$ , which is not necessarily correct.

In this work, we provided an exact characterization of CEPD effects in the interaction between circularly polarized few-cycle pulses and multielectron atoms and molecules including full account of the spatial dependence of the field (non-dipole effects). For systems which are invariant to rotations around the propagation direction of the field, a change of the CEPD corresponds to a rotation of the systems. For rotationally non-invariant systems, true non-geometrical CEPD effects may be observed. Calculations on H(1s) quantified the effects, and showed that observation of the momentum distribution can be used to measure CEPD for a circularly polarized laser pulse. For linearly polarized fields, the electrons spectrum was interpreted in terms of a classical model.

There is currently considerable interest in control of the response of atoms and small molecules to a strong few-cycle pulse [4], e.g., in connection with alignment dependent high-harmonic generation from small molecules [25, 26]. Here the harmonics provide a delicate probe of the molecular wave packet dynamics and,

in turn, steering the electronic wave packets controls the harmonics. The carrier-envelope-phase difference is one of the essential control parameters in few-cycle pulse and attosecond science.

We thank T.K. Kjeldsen and U.V. Poulsen for useful discussion. L.B.M. was supported by the Danish Natural Science Research Council (Grant No. 21-03-0163) and the Danish Research Agency (Grant. No. 2117-05-0081).

- 
- [1] T. Brabec and F. Krausz, *Rev. Mod. Phys.* **72**, 545 (2000).
  - [2] A. H. Zewail, *J. Phys. Chem.* **100**, 12701 (1996).
  - [3] P. H. Buckbaum, *Nature* **421**, 593 (2003).
  - [4] A. Scrinzi, M. Y. Ivanov, R. Kienberger, and D. M. Villeneuve, *J. Phys. B* **39**, R1 (2006).
  - [5] J. Itatani, F. Quere, G. L. Yudin, M. Y. Ivanov, F. Krausz, and P. B. Corkum, *Phys. Rev. Lett.* **88**, 173903 (2002).
  - [6] A. D. Bandrauk, S. Chelkowski, and N. H. Shon, *Phys. Rev. Lett.* **89**, 283903 (2002).
  - [7] E. Goulielmakis, M. Uiberacker, R. Kienberger, A. Baltuska, V. Yakovlev, A. Scrinzi, T. Westerwalbesloh, U. Keineberg, U. Heinzmann, M. Drescher, et al., *Science* **305**, 1267 (2004).
  - [8] E. Cormier and P. Lambropoulos, *Eur. Phys. J. D* **2**, 15 (1998).
  - [9] P. Dietrich, F. Krausz, and P. B. Corkum, *Opt. Lett.* **25**, 16 (2000).
  - [10] J. P. Hansen, J. Lu, L. B. Madsen, and H. Nilsen, *Phys. Rev. A* **64**, 033418 (2001).
  - [11] S. Chelkowski and A. D. Bandrauk, *Phys. Rev. A* **65**, 061802 (2002).
  - [12] D. B. Milošević, G. G. Paulus, and W. Becker, *Phys. Rev. Lett.* **89**, 153001 (2002).
  - [13] S. X. Hu and L. A. Collins, *Phys. Rev. A* **73**, 023405 (2006).
  - [14] V. Roudnev, B. D. Esry, and I. Ben-Itzhak, *Phys. Rev. Lett.* **93**, 163601 (2004).
  - [15] A. de Bohan, P. Antoine, D. B. Milošević, and B. Piraux, *Phys. Rev. Lett.* **81**, 1837 (1998).
  - [16] G. G. Paulus, F. Grasbon, H. Walther, P. Villoresi, M. Nisoli, S. Stagira, E. Priori, and D. D. Silvestri, *Nature* **414**, 182 (2001).
  - [17] A. Baltuska, T. Udem, M. Uiberacker, M. Hentschel, E. Goulielmakis, C. Gohle, R. Holzwarth, V. S. Yakovlev, A. Scrinzi, T. W. Hänsch, et al., *Nature* **421**, 611 (2003).
  - [18] G. G. Paulus, F. Lindner, H. Walther, A. Baltuska, E. Goulielmakis, M. Lezius, and F. Krausz, *Phys. Rev. Lett.* **91**, 253004 (2003).
  - [19] I. J. Sola, E. Mével, L. Elouga, E. Constant, V. Strelkov, P. Poletto, P. Villoresi, E. Benedetti, J.-P. Caumes, S. Stagira, et al., *Nature Physics (London)* **2**, 319 (2006).
  - [20] T. Remetter, P. Johnsson, J. Mauritsson, K. Varjú, Y. Ni, F. Lépine, E. Gustafsson, M. Kling, J. Khan, R. López-Martens, et al., *Nature Physics (London)* **2**, 323 (2006).
  - [21] P. Schlup, P. R. Eckle, A. Aghajani-Talesh, J. Biegert, M. P. Smolarski, A. Staudte, M. Schöffler, O. Jagutzki, R. Dörner, and U. Keller, in *Conference on Lasers and Electro-Optics (CLEO 06)* (2006).
  - [22] J. J. Sakurai, *Modern Quantum Mechanics* (Addison-Wesley Publishing Company, 1994).
  - [23] L. V. Keldysh, *J. Exptl. Phys. [Sov. Phys. JETP]* **47 (20)**, 1945 (1307) (1964 (1965)).
  - [24] G. Duchateau, E. Cormier, and R. Gayet, *Phys. Rev. A* **66**, 023412 (2002).
  - [25] T. Kanai, S. Minemoto, and H. Sakai, *Nature* **435**, 470 (2005).
  - [26] J. Itatani, D. Ziedler, J. Levesque, M. Spanner, D. M. Villeneuve, and P. B. Corkum, *Phys. Rev. Lett.* **94**, 123902 (2005).

# Symmetry of carrier-envelope phase difference effects in strong-field, few-cycle ionization of atoms and molecules

Christian Per Juul Martiny and Lars Bojer Madsen

*Department of Physics and Astronomy, University of Aarhus, 8000 Århus C, Denmark*

(Dated: July 28, 2018)

In few-cycle pulses, the exact value of the carrier-envelope phase difference (CEPD) has a pronounced influence on the ionization dynamics of atoms and molecules. We show that for atoms in circularly polarized light, a change in the CEPD is mapped uniquely to an overall rotation of the system, and results for arbitrary CEPD are obtained by rotation of the results from a single calculation with fixed CEPD. For molecules this is true only for linear molecules aligned parallel with the propagation direction of the field. The effects of CEPD are classified as geometric or non-geometric. The observations are exemplified by strong-field calculations on hydrogen.

PACS numbers: 32.80.Rm, 33.80.Rv, 42.50.Hz.

Nowadays, it is possible to construct and control intense laser pulses with only a few optical cycles [1], i.e., pulses described by a vector potential of the form  $\vec{A}(t) = A_0 f(t) \sin(\omega(t - \frac{\tau}{2}) + \phi) \hat{e}$ , where  $A_0$  is the amplitude,  $f(t)$  is the envelope,  $\tau$  is the pulse length,  $\omega$  is the frequency,  $\phi$  is the carrier-envelope phase difference (CEPD), and  $\hat{e}$  is the polarization vector. The corresponding electric field is obtained from the vector potential by  $\vec{E}(t) = -\partial_t \vec{A}(t)$ , and is shown in Fig. 1 for a  $\sin^2$  envelope. Such pulses can be used to probe molecular and atomic dynamics on a very short time scale [2, 3]. The associated ionization dynamics becomes sensitive to the exact shape of the pulse and the carrier-envelope phase difference (CEPD) (see Fig. 1). This dependence may be understood by the exponential dependence of the ionization rate on the instantaneous field strength and the corresponding emergence of the electron into the field-dressed continuum at specific instants of time during the pulse [4]. Asymmetries in the photoelectron spectrum may give information about the CEPD, and hence help in the characterization of the field. Electrons released at different times are accelerated to different final momenta and this fact is exploited in attosecond streaking [5] to map the time distribution of the pulse into a momentum distribution of the photoelectron, and to characterize the ultra-fast pulses [6]. Hence, just as few-cycle pulses are diagnostic tools for atoms and small molecules, the very same systems serve as diagnostic tools for the pulses themselves [7]. The latter statement, of course, assumes that an accurate theoretical description is at hand for the pulsed laser-matter interaction. It is the purpose of this work to add further to this understanding. In particular we are concerned with the CEPD effects, and a geometric interpretation of these.

Carrier-envelope phase difference effects were studied theoretically with emphasis on CEPD-induced spatial asymmetries in the ATI-spectrum/angular distribution in a number of papers on strong-field ionization of atoms [8, 9, 10, 11, 12] and molecules [13], strong-field dissociation [14], and high-harmonic generation [15]. The

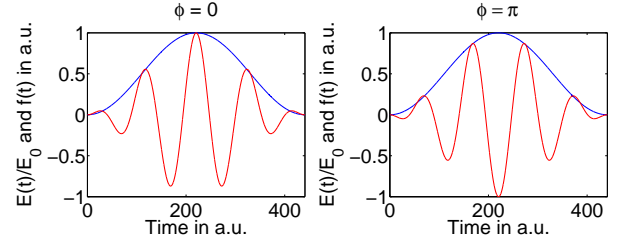


FIG. 1: (Color online). The electric field  $E(t)/E_0$ , normalized to the peak field strength  $E_0$  and the pulse envelope  $f(t)$  as a function of time for two values of the CEPD,  $\phi$ . The electric field points in opposite directions for  $\phi = 0$  and  $\phi = \pi$ . In ionization, the electric field will shake the electron until it gains enough energy to escape the Coulomb potential, and the angular distribution will depend on CEPD because the electric field (and the force  $\vec{F} = -\vec{E}$ ) points in opposite directions for  $\phi = 0$  and  $\phi = \pi$ . The field parameters are  $\tau = 441$  a.u. and  $\omega = 0.057$  a.u. (800 nm).

asymmetries can be used to extract information about and ultimately to measure the CEPD. In Ref. [16] a spatial asymmetry in ionization with few-cycle circular polarized laser pulses was observed for the first time. In Ref. [17] the generation of intense few-cycle laser pulses with stable CEPD was demonstrated, and a way of measuring CEPD, based on soft-X-ray radiation was presented. In Ref. [18] a spatial asymmetry in the ionization with few-cycle linear polarized laser pulses was measured, and the CEPD was determined with an estimated error of  $\pi/10$ . Asymmetries in the ionization signal combined with an attosecond pump pulse [6] were used to measure directly the field of a linearly polarized few-cycle pulse [7]. Very recently, the detailed control over the CEPD played a crucial role in attosecond electron dynamics [18, 19, 20], and experiments supporting the present findings have been reported at conferences [21].

In this work, we present a systematic theoretical study of the symmetry of the response of atomic and molecular systems under a change of the CEPD in few-cycle pulses,

and we exemplify the discussion with a study of the differential electron momentum distribution for hydrogen under such pulses.

We start out by considering an  $n$ -electron atom interacting with a few-cycle circularly polarized laser pulse described by the vector potential

$$\vec{A}(\phi, t, \vec{r}) = \frac{A_0}{\sqrt{2}} f(\eta) \times \left( \cos(\eta + \phi + \frac{\pi}{2}) \vec{e}_x + \sin(\eta + \phi + \frac{\pi}{2}) \vec{e}_y \right), \quad (1)$$

with  $f(\eta) = \sin^2(\frac{\eta}{2N})$  the envelope,  $N$  the number of optical cycles,  $\eta = \omega t - k z$ ,  $\omega$  the frequency, and  $\vec{k} = k \vec{e}_z$  the wave vector. In the present case, with full inclusion of the spatial dependence of the field, the interaction of the atom with the field is obtained by the minimal coupling  $\hat{p} \rightarrow \hat{p} + \vec{A}$  and the time-dependent Schrödinger equation reads [atomic units (a.u.) with  $m_e = e = a_0 = \hbar = 1$  are used throughout],

$$i \frac{\partial}{\partial t} \Psi = \left( H_0 + \sum_{j=1}^n \vec{A}(\phi, t, \vec{r}_j) \cdot \hat{p}_j + \frac{n A_0^2}{4} f^2(\eta) \right) \Psi, \quad (2)$$

where  $H_0$  is the field-free Hamiltonian. We are interested in relating this equation to an equation for the  $\phi = 0$  case. To this end, we note that the unitary operator  $D(\phi) = \exp(i J_z \phi)$ , where  $J_z$  is the total angular momentum, corresponds to a rotation of our system by an angle  $-\phi$  around the  $z$ -axis. Since  $H_0$  is invariant under rotations around the  $z$ -axis, the transformed wave function  $\Psi' = D(\phi) \Psi$  satisfies the Schrödinger equation,

$$i \frac{\partial}{\partial t} \Psi' = \left( H_0 + \sum_{j=1}^n D(\phi) \vec{A}(\phi, t, \vec{r}_j) \cdot \hat{p}_j D^\dagger(\phi) + \frac{n A_0^2}{4} D(\phi) f^2(\eta) D^\dagger(\phi) \right) \Psi', \quad (3)$$

and using the Baker-Hausdorff lemma [22] we obtain,

$$i \frac{\partial}{\partial t} \Psi' = \left( H_0 + \sum_{j=1}^n \vec{A}(0, t, \vec{r}_j) \cdot \hat{p}_j + \frac{n A_0^2}{4} f^2(\eta) \right) \Psi'. \quad (4)$$

When we compare (2) and (4), we see that a change in the CEPD from  $\phi = 0$  to  $\phi = \phi'$  corresponds to a rotation of our system around the  $z$ -axis by the angle  $\phi'$ . This fact is not only theoretically interesting, but also helpful in practical calculations since this symmetry property reduces the number of computations one has to perform to a single one – all other results are obtained by suitable rotations. For instance, imagine we are interested in the differential ionization probability  $\frac{dP_{fi}}{dq_x dq_y}(\phi)$  for the momenta  $q_x, q_y$  in the polarization plane and for a general  $\phi > 0$ . Then we calculate  $\frac{dP_{fi}}{dq_x dq_y}(\phi = 0)$ , and rotate the result counterclockwise by an angle  $\phi$  to obtain  $\frac{dP_{fi}}{dq_x dq_y}(\phi)$ .

In the above derivation it is essential that the field-free Hamiltonian  $H_0$  is invariant to rotations around the  $z$ -axis. If this is not the case, the proof breaks down. As an example we look at ionization of diatomic molecules, or more generally linear molecules, in circularly polarized few-cycle laser pulses. If the molecule is aligned along the laser propagation direction, then the field-free Hamiltonian still has the required symmetry and the theorem holds. If the molecule is not aligned along this axis, the system does not have the required symmetry and CEPD effects can not be reduced to a geometrical rotation. Accordingly, we may make a distinction between rotational invariant atomic and molecular systems where the CEPD effects are purely geometric rotations, and systems which are not rotational invariant in which case true *non-geometrical* CEPD effects occur. For example, the results on strong-field ionization of  $K_2^+$  with the molecule in the polarization plane [13] belong to the latter category.

As an illustration of the present findings, we consider ionization of atomic hydrogen,  $H(1s)$ , in the strong-field approximation (SFA) [23]. We assume the dipole approximation which means that  $\eta = \omega t$  in (1) and use that  $\vec{E} = -\partial_t \vec{A}$ . The probability amplitude for direct ionization reads

$$T_{fi} = -i \int_0^\tau \langle \Psi_f(\vec{r}, t) | \vec{E} \cdot \vec{r} | \Psi_i(\vec{r}, t) \rangle dt, \quad (5)$$

where  $\Psi_i(\vec{r}, t)$  is the  $1s$  ground state wave function. The final state  $\Psi_f(\vec{r}, t)$  is represented by a Coulomb-Volkov wave function [24] with asymptotic momentum  $\vec{q}$ . The integral in (5) is analyzed as in [24] and the numerical evaluation is performed with Gauss-Legendre quadrature. By exploiting the invariance of the dot-product under rotations ( $\vec{E}(\phi) \cdot \vec{r} = [R_z(\phi) \vec{E}(\phi = 0)] \cdot [R_z(\phi) R_z(-\phi) \vec{r}] = \vec{E}(\phi = 0) \cdot \vec{r}'$ , where  $R_z(\phi)$  is the  $3 \times 3$  matrix describing rotations around the  $z$  axis), the SFA is readily shown to respond to CEPD changes like the exact theory discussed above.

Once  $T_{fi}$  is known, a simple numerical integration over  $q_z$  gives us the  $(q_x, q_y)$  distribution  $\frac{dP_{fi}}{dq_x dq_y} = \int |T_{fi}|^2 dq_z$ . Figure 2 presents the calculated distribution for various values of  $\phi$ . For varying  $\phi$ , the distribution rotates in accordance with the general theory. For  $\phi = 0$ ,  $\frac{dP_{fi}}{dq_x dq_y}$  has a peak around  $(q_x = 0, q_y \sim 0.6)$  (this peak corresponds to about 14 photons above threshold), and is almost symmetric around the line  $q_x = 0$ . As  $\phi$  increases, this line is turned counterclockwise, so that  $\frac{dP_{fi}}{dq_x dq_y}$  has a peak around  $(q_y = 0, q_x \sim -0.6)$  for  $\phi = \frac{\pi}{2}$ .

Some of the features can be explained by a semiclassical two-step model [11]: first the electron escapes to the continuum at  $t = t_0$  with velocity  $\vec{v}(t_0) = \vec{0}$ . Second, it moves like a classical particle under the influence of the external Coulomb and laser fields. If, we neglect the Coulomb potential, which is justified if the



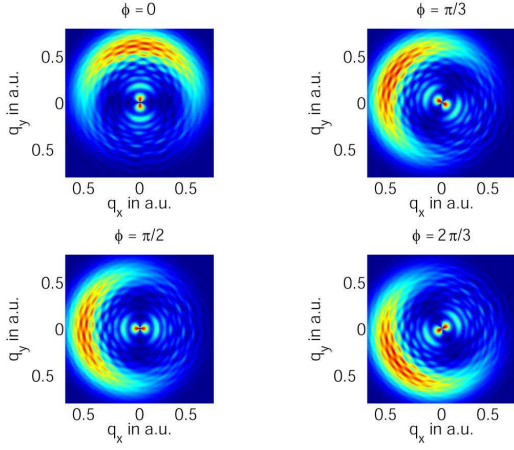


FIG. 2: (Color online) The  $(q_x, q_y)$  distribution for strong-field ionization of H(1s) for various values of  $\phi$ , with  $I = 5.0 \times 10^{13} \text{ W/cm}^2$ ,  $\omega = 0.057$  corresponding to a central wavelength of 800nm and three cycles,  $N = 3$ . The grid size is  $dq_x = dq_y = 0.01$ .

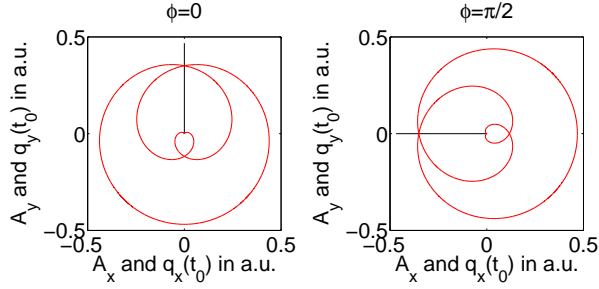


FIG. 3: The curves show the time-dependent vector potential and the lines show  $\vec{q}^d$  for  $\phi = 0, \pi/2$ . Laser parameters are as in Fig. 2.

field is very strong, Newton's second law tells us that  $q_x(t) = A_x(t) + q_x^d$ ,  $q_y(t) = A_y(t) + q_y^d$  where  $q_x^d = -A_x(t_0)$  and  $q_y^d = -A_y(t_0)$ . This means that the photoelectron direction, after the pulse where  $\vec{A}$  vanishes, is determined by the vector  $\vec{q}^d = (q_x^d, q_y^d)$ . For simplicity  $t_0$  is chosen to be  $\tau/2$ , which is the time when  $|\vec{E}(t)|$  reaches its maximum. Figure 3 shows plots of the time-dependent vector potential and  $\vec{q}^d = -\vec{A}(t_0)$  for various values of  $\phi$ . The model explains how the preferred direction (the line of symmetry) of the photoelectron depends on CEPD.

Finally we consider the case of a linearly polarized laser field and return to the question of symmetry. The vector potential in the linear case,  $\vec{A}(\phi, t, \vec{r}) = A_0 f(\eta) \sin(\eta + \phi + \pi/2) \hat{e}_y$ , can be written as  $\vec{A}(\phi, t, \vec{r}) = \frac{1}{\sqrt{2}} (\vec{A}_L(\phi, t) - \vec{A}_R(\phi, t))$ , where  $\vec{A}_{L/R}(\phi, t, \vec{r}) = \frac{A_0}{\sqrt{2}} f(\eta) (\cos(\eta + \phi + \pi/2) \hat{e}_x \pm \sin(\eta + \phi + \pi/2) \hat{e}_y)$  describe left (+) and right (-) hand circularly polarized fields. This relation suggests that we can characterize CEPD effects for a linearly po-

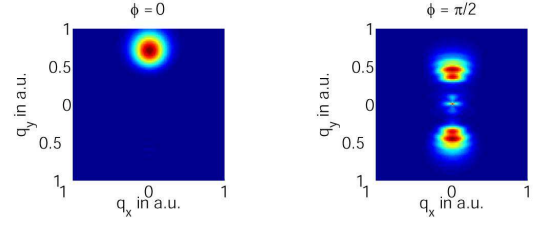


FIG. 4: (Color online) The  $(q_x, q_y)$  distribution for strong-field ionization of H(1s) by a linearly polarized field for  $\phi = 0, \pi/2$ , with  $I = 5.0 \times 10^{13} \text{ W/cm}^2$ ,  $\omega = 0.057$  corresponding to a central wavelength of 800nm and three cycles,  $N = 3$ . The grid size is  $dq_x = dq_y = 0.02$ .

larized pulse similarly to circularly polarized pulses. Unfortunately, in exact theory, it is not possible to separate the effects of the circularly polarized fields, since they do not individually commute with the field-free Hamiltonian.

Figure 4 shows two examples for a linear field corresponding to the  $\phi = 0$  and  $\phi = \pi/2$  cases. These results may be interpreted in terms of the classical model discussed above ( $q_y = -A_y(t_0)$ ). For  $\phi = 0$ , we have the peak of the field at the peak of the envelope and this produces electrons with positive momentum,  $q_y = -A_y(\frac{\tau}{2})$ . For  $\phi = \pi/2$ , the vector potential is antisymmetric with respect to the peak of the envelope, and the electron spectrum reflects this in a forward-backward symmetry. For  $\phi = \pi/2$ , the spectrum has moved to smaller momenta since the two maxima of the vector potential are lower in this case. Notice, however, that the model can not explain the size of the shift. There are two reasons for this discrepancy. First, the model neglects the Coulomb potential. Second we assume that  $v_0 = 0$ , which is not necessarily correct.

In this work, we provided an exact characterization of CEPD effects in the interaction between circularly polarized few-cycle pulses and multielectron atoms and molecules including full account of the spatial dependence of the field (non-dipole effects). For systems which are invariant to rotations around the propagation direction of the field, a change of the CEPD corresponds to a rotation of the systems. For rotationally non-invariant systems, true non-geometrical CEPD effects may be observed. Calculations on H(1s) quantified the effects, and showed that observation of the momentum distribution can be used to measure CEPD for a circularly polarized laser pulse. For linearly polarized fields, the electrons spectrum was interpreted in terms of a classical model.

There is currently considerable interest in control of the response of atoms and small molecules to a strong few-cycle pulse [4], e.g., in connection with alignment dependent high-harmonic generation from small molecules [25, 26]. Here the harmonics provide a delicate probe of the molecular wave packet dynamics and,

in turn, steering the electronic wave packets controls the harmonics. The carrier-envelope-phase difference is one of the essential control parameters in few-cycle pulse and attosecond science.

We thank T.K. Kjeldsen and U.V. Poulsen for useful discussion. L.B.M. was supported by the Danish Natural Science Research Council (Grant No. 21-03-0163) and the Danish Research Agency (Grant. No. 2117-05-0081).

- 
- [1] T. Brabec and F. Krausz, *Rev. Mod. Phys.* **72**, 545 (2000).
  - [2] A. H. Zewail, *J. Phys. Chem.* **100**, 12701 (1996).
  - [3] P. H. Buckbaum, *Nature* **421**, 593 (2003).
  - [4] A. Scrinzi, M. Y. Ivanov, R. Kienberger, and D. M. Villeneuve, *J. Phys. B* **39**, R1 (2006).
  - [5] J. Itatani, F. Quere, G. L. Yudin, M. Y. Ivanov, F. Krausz, and P. B. Corkum, *Phys. Rev. Lett.* **88**, 173903 (2002).
  - [6] A. D. Bandrauk, S. Chelkowski, and N. H. Shon, *Phys. Rev. Lett.* **89**, 283903 (2002).
  - [7] E. Goulielmakis, M. Uiberacker, R. Kienberger, A. Baltuska, V. Yakovlev, A. Scrinzi, T. Westerwalbesloh, U. Keineberg, U. Heinzmann, M. Drescher, et al., *Science* **305**, 1267 (2004).
  - [8] E. Cormier and P. Lambropoulos, *Eur. Phys. J. D* **2**, 15 (1998).
  - [9] P. Dietrich, F. Krausz, and P. B. Corkum, *Opt. Lett.* **25**, 16 (2000).
  - [10] J. P. Hansen, J. Lu, L. B. Madsen, and H. Nilsen, *Phys. Rev. A* **64**, 033418 (2001).
  - [11] S. Chelkowski and A. D. Bandrauk, *Phys. Rev. A* **65**, 061802 (2002).
  - [12] D. B. Milošević, G. G. Paulus, and W. Becker, *Phys. Rev. Lett.* **89**, 153001 (2002).
  - [13] S. X. Hu and L. A. Collins, *Phys. Rev. A* **73**, 023405 (2006).
  - [14] V. Roudnev, B. D. Esry, and I. Ben-Itzhak, *Phys. Rev. Lett.* **93**, 163601 (2004).
  - [15] A. de Bohan, P. Antoine, D. B. Milošević, and B. Piraux, *Phys. Rev. Lett.* **81**, 1837 (1998).
  - [16] G. G. Paulus, F. Grasbon, H. Walther, P. Villoresi, M. Nisoli, S. Stagira, E. Priori, and D. D. Silvestri, *Nature* **414**, 182 (2001).
  - [17] A. Baltuska, T. Udem, M. Uiberacker, M. Hentschel, E. Goulielmakis, C. Gohle, R. Holzwarth, V. S. Yakovlev, A. Scrinzi, T. W. Hänsch, et al., *Nature* **421**, 611 (2003).
  - [18] G. G. Paulus, F. Lindner, H. Walther, A. Baltuska, E. Goulielmakis, M. Lezius, and F. Krausz, *Phys. Rev. Lett.* **91**, 253004 (2003).
  - [19] I. J. Sola, E. Mével, L. Elouga, E. Constant, V. Strelkov, P. Poletto, P. Villoresi, E. Benedetti, J.-P. Caumes, S. Stagira, et al., *Nature Physics (London)* **2**, 319 (2006).
  - [20] T. Remetter, P. Johnsson, J. Mauritsson, K. Varjú, Y. Ni, F. Lépine, E. Gustafsson, M. Kling, J. Khan, R. López-Martens, et al., *Nature Physics (London)* **2**, 323 (2006).
  - [21] P. Schlup, P. R. Eckle, A. Aghajani-Talesh, J. Biegert, M. P. Smolarski, A. Staudte, M. Schöffler, O. Jagutzki, R. Dörner, and U. Keller, in *Conference on Lasers and Electro-Optics (CLEO 06)* (2006).
  - [22] J. J. Sakurai, *Modern Quantum Mechanics* (Addison-Wesley Publishing Company, 1994).
  - [23] L. V. Keldysh, *J. Exptl. Phys. [Sov. Phys. JETP]* **47 (20)**, 1945 (1307) (1964 (1965)).
  - [24] G. Duchateau, E. Cormier, and R. Gayet, *Phys. Rev. A* **66**, 023412 (2002).
  - [25] T. Kanai, S. Minemoto, and H. Sakai, *Nature* **435**, 470 (2005).
  - [26] J. Itatani, D. Ziedler, J. Levesque, M. Spanner, D. M. Villeneuve, and P. B. Corkum, *Phys. Rev. Lett.* **94**, 123902 (2005).